J Membrane Biol (2008) 222:107–113
DOI 10.1007/s00232-008-9100-1

ORIGINAL ARTICLES

ATP Dependence of Na^+-Driven $Cl–HCO_3$ Exchange in Squid Axons

Bruce A. Davis · Emilia M. Hogan · John M. Russell · Walter F. Boron

Received: 17 September 2007 / Accepted: 21 February 2008 / Published online: 14 May 2008

Abstract Squid giant axons recover from acid loads by activating a Na^+-driven $Cl–HCO_3$ exchanger. We internally dialyzed axons to an intracellular pH (pH_i) of 6.7, halted dialysis and monitored the pH_i recovery (increase) in the presence of ATP or other nucleotides, using cyanide to block oxidative phosphorylation. We computed the equivalent acid-extrusion rate (J_H) from the rate of pH_i increase and intracellular buffering power. In experimental series 1, we used dialysis to vary $[ATP]_i$, finding that Michaelis-Menten kinetics describes J_H vs. $[ATP]_i$, with an apparent V_{max} of 15.6 pmole cm^{-2} s^{-1} and K_m of 124 μM. In series 2, we examined ATPγS, AMP-PNP, AMP-PCP, AMP-CPP, GMP-PNP, ADP, ADPβS and GDPβS to determine if any, by themselves, could support transport. Only ATPγS (8 mM) supported acid extrusion; ATPγS also supported the HCO_3^--dependent ^{36}Cl efflux expected of a Na^+-driven $Cl–HCO_3$ exchanger. Finally, in series 3, we asked whether any nucleotide could alter J_H in the presence of a background $[ATP]_i$ of ~230 μM (control J_H = 11.7 pmol cm^{-2} s^{-1}). We found J_H was decreased modestly by 8 mM AMP-PNP (J_H = 8.0 pmol cm^{-2} s^{-1}) but increased modestly by 1 mM ADPβS (J_H = 16.0 pmol cm^{-2} s^{-1}). We suggest that ATPγS leads to stable phosphorylation of the transporter or an essential activator.

Keywords Intracellular pH · Nucleotide analog · Dialysis · Kinetics

B. A. Davis · E. M. Hogan · W. F. Boron
Department of Cellular and Molecular Physiology, Yale University School of Medicine, New Haven, CT 06520, USA

J. M. Russell
Department of Biology, Syracuse University, Syracuse, NY 13244, USA

W. F. Boron (✉)
Department of Physiology and Biophysics, Case Western Reserve University School of Medicine, 10900 Euclid Avenue, Cleveland, OH 44106-4970, USA
e-mail: walter.boron@case.edu; walter.boron@yale.edu

Introduction

Sodium-driven $Cl–HCO_3$ exchange is the predominant acid-extrusion mechanism in axons from the squid *Loligo pealei*. The transporter, which is blocked by stilbene derivatives such as 4-acetamido-4′-isothiocyanatostilbene-2,2′-disulfonate (SITS) and 4,4′-diisothiocyanatostilbene-2,2′-disulfonate (DIDS), exchanges intracellular Cl^- for extracellular Na^+ and an HCO_3^--related species (Russell and Boron 1976; Thomas 1976, 1977; Boron and De Weer 1976a; Boron and Russell 1983). In the squid axon, this transporter has an absolute requirement for ATP (Boron and De Weer 1976a). In principle, the transporter could require ATP either as a fuel or as a cofactor. The fuel hypothesis, which predicts that the ATP is stoichiometrically hydrolyzed, seems unlikely inasmuch as the Na^+ gradient has sufficient energy to support transport (Boron 1989). The final evidence against the fuel hypothesis is that internally dialyzing an axon with adenosine 5′-(γ-thio) triphosphate (ATPγS), rather than ATP, at low intracellular pH (pH_i) supports transport, even after the subsequent washout of ATPγS (Russell and Boron 1976). However, after preactivation of the transporter with ATPγS at low pH_i, raising pH_i causes gradual inactivation.

Although these data rule out the fuel hypothesis, they do not address the issue of whether ATP is required to bind to the transporter (or an essential activator) or to phosphorylate it. In principle, this question could be approached by

examining whether ATP analogues such as adenosine 5′-(β,γ-methylene)triphosphate (AMP-PCP, in which a methylene group links the β and γ phosphates) and adenosine 5′-(β,γ-imido)triphosphate (AMP-PNP, with an imido linkage)—which cannot serve as substrates for protein kinases—can support transport.

In the present study, we internally dialyzed squid axons to a low pH_i (6.7), halted dialysis and exposed the axons to CO_2/HCO_3^-, and then computed the equivalent acid-extrusion rate (J_H) from the rate of pH_i recovery from this acid load. In one series of experiments, in which we used dialysis to vary $[ATP]_i$, we found that simple Michaelis-Menten kinetics describes the dependence of J_H on $[ATP]_i$, with an apparent J_{max} of 15.6 pmol cm^{-2} s^{-1} and an apparent K_m of 124 μM. In a second series of experiments, we examined axons dialyzed with a variety of nucleotides to determine if any could support transport in the absence of ATP. We found that only ATPγS supported a statistically significant level of transport. Moreover, as expected for a Na^+-driven Cl-HCO_3 exchanger, ATPγS supported HCO_3^--stimulated ^{36}Cl efflux. Finally, in a third series of experiments, we asked whether the nucleotides could alter J_H in the presence of a background $[ATP]_i$ of ~230 μM (control J_H = 11.7 pmol cm^{-2} s^{-1}). We found that 8 mM AMP-PNP modestly decreased transport (J_H = 8.0 pmol cm^{-2} s^{-1}), whereas 1 mM ADPβS modestly increased it (J_H = 16.0 pmol cm^{-2} s^{-1}). Thus, the apparent affinity of Na^+-driven Cl–HCO_3 exchange for ATP is similar to that of other ATP-dependent processes, and no nucleotide other than ATPγS could support transport in the absence of ATP.

Methods

General

The experiments were conducted at the Marine Biological Laboratory (Woods Hole, MA). Technical details have been described previously (Boron and Russell 1983; Boron 1985; Boron and Knakal 1989). Briefly, a 3–4 cm length of giant axon (400–700 μm in diameter) was dissected from the squid *L. pealei* and horizontally cannulated in a chamber designed for internal dialysis (Brinley and Mullins 1967). Cellulose acetate dialysis tubing (outer diameter 140 μm) was threaded down the length of the axon and perfused with a dialysis fluid (DF) at ~2.1 μl/min. Also inserted into the axon through opposite cannulas were a pH-sensitive microelectrode (Hinke 1967) and an internal reference microelectrode (filled with 3 M KCl). Details on microelectrode construction, use of high-impedance electrometers and other devices to handle electrode signals, computer acquisition of data and computer control of the experiments have been described elsewhere (Boron and Russell 1983; Boron 1985).

Solutions

Artificial seawaters

The standard HCO_3^--free artificial seawater (ASW) had the following composition (in mM): 425.2 Na^+, 12 K^+, 3 Ca^+, 52.5 Mg^{2+}, 521 Cl^-, 5 anionic form of [2-hydroxyethyl]-1-piperazine-propane sulfonic acid (EPPS) and 5 neutral form of EPPS (pK ~ 8.0), 0.1 $EDTA^=$, 1 CN^-. The HCO_3^-–containing ASW was made by replacing 12 mM KCl with 12 mM $KHCO_3$ and equilibrating with 0.5% CO_2, 99.5% O_2. Moreover, in this HCO_3^-–containing ASW, the EPPS concentration was raised to 30 mM, with corresponding reductions in $[Mg^{2+}]$ and $[Cl^-]$ to keep osmolarity constant. All solutions were titrated to pH 8.0 using NaOH or HCl. Osmolarity was adjusted to 965–970 mOsm/kg using mannitol or H_2O.

Dialysis fluids

The standard DF for acid loading had the following composition (in mM): 0 Na^+, 413.3 K^+, 400 Cl^-, 14 glutamate, 13.3 anionic form of (2–9*N*-morpholino)-ethanesulfonic acid (MES), 13.3 neutral form of MES and 0.5 phenol red. The fluid was adjusted to pH 6.7 with NMDG base or HCl. Osmolarity was adjusted to 965–970 mOsm/kg using glycine or H_2O.

We varied the [total Mg^{2+}] in the DFs according to the formula [nucleotide] + 3 mM = [total Mg^{2+}]. Because the nucleotides bind Mg^{2+} in a ~1:1 ratio, this provision should maintain an approximately constant free $[Mg^{2+}]_i$. To achieve the desired final [total Mg^{2+}] in the DF (i.e., 0, 3, 4, 7, 8 and 11 mM), we mixed Mg^{2+}-free DF with DF containing 25 mM Mg^{2+}.

An ATP-buffered DF containing 4 mM ATP and 3 mM PEPPA (Altamirano et al. 1995) was made by adding aliquots from stock solution containing 400 mM ATP as well as a stock solution containing 300 mM phosphoenolpyruvate (PEP) plus 300 mM phosphoarginine (PA) to an ATP-free stock DF. Similarly, DFs with a range of [ATP] values plus a constant 3 mM PEPPA were made by mixing a DF containing 4 mM ATP/3 mM PEPPA with an ATP-free DF containing 3 mM PEPPA. Finally, we generated ATP-free DFs with a range of [PEPPA] values by mixing an ATP-free DF containing 3 mM PEPPA with an ATP-free/PEPPA-free DF. All of the DFs used for the $[ATP]_i$ dose–response curve were titrated to a pH of 6.7. We obtained all nucleotides from Sigma Aldrich (St. Louis, MO). ATPγS, AMP-PNP, adenosine 5′-(α,β-methylene)triphosphate (AMP-CPP) and AMP-PCP were present at a final concentration of 8 mM in the DFs. ADP, adenosine 5′-(β-thio)diphosphate (ADPβS), guanosine 5′-(β,γ-imido)triphosphate (GMP-PNP) and

guanosine 5′-(β-thio)diphosphate (GDPβS) were present at a final concentration of 1 mM.

Measurement of Intracellular ATP

We assayed ATP concentrations as described previously (Altamirano et al. 1988). Briefly, previously dialyzed axons were cut at both cannulated ends and placed on small pieces of Parafilm® (Alcan, Neenah, WI) using sharp forceps. The axoplasm was then squeezed from the axon using a device similar to a miniature paint roller. After rapidly weighing the Parafilm with the axoplasm, we transferred the Parafilm containing the axoplasm to a glass tube containing a stop buffer (0.3 N perchloric acid, subsequently neutralized with 0.25 M KOH, 0.15 M 3-[*N*-morpholino]propanesulfonic acid [MOPS] and 0.15 KCl) and stored the material until the time of assay. ATP was measured using the firefly luciferin-luciferase assay kit (LKB Wallach, Turku, Finland). The principle of the assay is based on the firefly luciferase-catalyzed oxidation of D-luciferin in the presence of an ATP-magnesium salt and O_2. The ATP can be quantified by the amount of light produced.

Calculation of Acid-Extrusion Rates

As described previously (Boron and Knakal 1985), pH_i data were acquired by computer, and rates of pH_i recovery from acid loads (dpH_i/dt) were determined from a linear curve fit to the data. Net J_H is defined as the net efflux of H^+ (or other acid) plus the net influx of HCO_3^- (or other base) and computed as the product of dpH_i/dt, total intracellular buffering power—assumed to be the sum of the closed-system buffering power computed for the DF and the open-system buffering power for CO_2/HCO_3^- (Roos and Boron 1981)—and volume-to-surface ratio.

Measurement of ^{36}Cl Efflux

Axons were prepared as described above and dialyzed with the appropriate DF for 60–90 min prior to changing to an identical DF containing ^{36}Cl (specific activity ≅ 0.25 μCi/μmol of Cl^-). The DF was the same as above but with 150 mM Cl^- rather than 400 mM Cl^- (glutamate replacing Cl^-). The ASW superfusing the axon was then collected and each timed sample counted using a liquid scintillation counter to an error of <5% (Altamirano et al. 1995).

Statistics

Values are reported as means ± standard errors. Groups of data were compared using one-way analysis of variance (ANOVA) followed by Dunnett's post hoc analysis, using KaleidaGraph® (Synergy Software, Reading, PA).

Results

Earlier experiments on intact (i.e., undialyzed) squid giant axons, acid-loaded by exposure to 5% CO_2, had shown that addition of cyanide to ASW blocks the pH_i recovery that we now know is mediated by the Na^+-driven $Cl–HCO_3$ exchanger (Boron and De Weer 1976a). Figure 1 shows an experiment on an axon that we internally dialyzed for ~60 min (segment *ab*) with a pH-6.7, Na^+-free DF that contained 8 mM ATP—a concentration that we used in an earlier study of ATPγS (Boron et al. 1988)—plus 3 mM PEPPA. The axon was superfused with the standard HCO_3^--free ASW containing 1 mM CN^- to block oxidative phosphorylation. When we halted dialysis (point *b*), intracellular pH stabilized and slowly increased as control of pH_i returned to the axon (*bc*). Exposing the axon to 12 mM HCO_3^-/0.5% CO_2 ASW resulted in a small, brief acidification (*cd*) caused by the influx of CO_2. The pH_i then recovered (i.e., increased) due to stimulation of Na^+-driven $Cl–HCO_3$ exchange (*de*). Addition of 0.5 mM SITS prevented any further pH_i increase (*ef*), as is expected of this transporter.

$[ATP]_i$ Dependence of Na-Driven $Cl–HCO_3$ Exchange

To determine the dose dependence of the ATP requirement of the Na^+-driven $Cl–HCO_3$ exchanger, we performed experiments similar to that shown in Fig. 1, except that we dialyzed the axons with DFs designed to achieve a broad

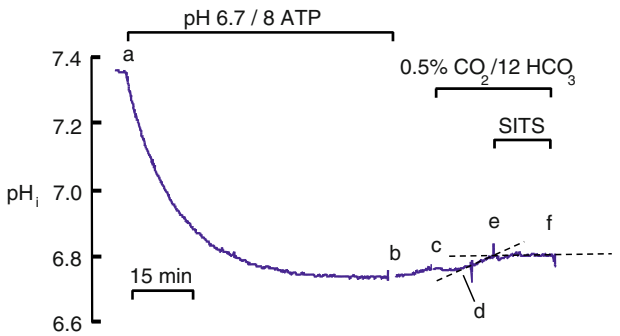

Fig. 1 Effect of dialysis with ATP on Na-driven $Cl–HCO_3$ exchange. Prior to the start of dialysis, pH_i was allowed to stabilize for several minutes. All ASWs contained 1 mM CN^-. At point *a*, we initiated dialysis with a pH-6.7 fluid that contained 8 mM ATP and continued dialyzing for ~1 h (segment *ab*). Dialysis was terminated at point *b*, returning control of pH_i to the axon (*bc*). At point *c*, the axon was exposed to ASW containing 12 mMHCO_3^- and gassed with 0.5% CO_2. At point *e*, we added 0.5 mM SITS. *Dashed lines* represent rates of pH_i change before and after application of SITS. We removed an electrical artifact at the break in the record at point *b*

Table 1 Measured [ATP] in axoplasm of axons dialyzed with various DFs[a]

Nominal composition of DF		[ATP] (μM)[b]	J_H (pmole cm^{-2} s^{-1})[b]
[ATP] (mM)	[PEPPA] (mM)		
0	0	11 ± 2 (10)	1.0 ± 0.5 (10)
0	0.375	45 ± 6 (8)	3.2 ± 0.6 (6)
0	0.750	94 ± 26 (12)	6.1 ± 1.1 (7)
0.125	3.0	185 ± 38 (4)	8.5 ± 1.4 (4)
0	1.5	205 ± 33 (5)	9.4 ± 1.9 (5)
0	3.0	231 ± 16 (7)	11.7 ± 0.8 (8)
0.250	3.0	235 ± 146 (2)	10.6 ± 1.1 (3)
0.500	3.0	503 ± 80.9 (3)	11.6 ± 1.2 (3)
1.0	3.0	1,047 ± 344 (2)	12.4 ± 1.6 (3)
4	3.0	1,463 ± 259 (3)	14.7 ± 1.5 (3)

[a] All ASWs contained 1 mM cyanide

[b] Mean ± SEM, number of analyses in parentheses

range of $[ATP]_i$ in the living axon. Because dialysis, by itself, is insufficient to reduce axoplasmic [ATP] to near-zero values—due to endogenous ATP production—we included 1 mM CN^- in the ASW. When we varied the added [ATP] of the DFs from 0 to 4 mM, we added 3 mM of the phosphagens (i.e., ATP buffers) PEP and PA in order to "clamp" axoplasmic [ATP] following cessation of dialysis. Pyruvate kinase converts PEP to pyruvate, simultaneously converting ADP to ATP. Similarly, arginine kinase converts PA to arginine, also simultaneously converting ADP to ATP. Finally, at the end of each pH_i experiment, we expressed the axoplasm and measured its [ATP]. Table 1 summarizes the directly measured ATP concentrations. Figure 2 summarizes the $[ATP]_i$ dependence of J_H. Note that the $[ATP]_i$ values in this plot are the measured values from Table 1, not the nominal $[ATP]_{DF}$. A nonlinear least-squares fitting procedure yielded an apparent K_m of 124 ± 19 μM and an apparent V_{max} of 15.6 ± 6.3 pmole cm^{-2} s^{-1}.

Effect of Nucleotides on Transport at Near-Zero Background ATP

To address the question of whether ATP is required for phosphorylation vs. binding, we surveyed eight nucleotide analogues for the ability to support transport at very low $[ATP]_i$ values. The protocol was identical to that for the axon represented in Fig. 1 except that the DF (1) was free of ATP and PEPPA and (2) contained either no nucleotide or one of the eight test nucleotide analogues. In the absence of any added nucleotide (i.e., actual $[ATP]_i$ = 11 μM), J_H (i.e., background flux) was 1.0 ± 0.5 (Fig. 3, leftmost bar and top data row in Table 1). Confirming the observation from a previous study, ATPγS supported a

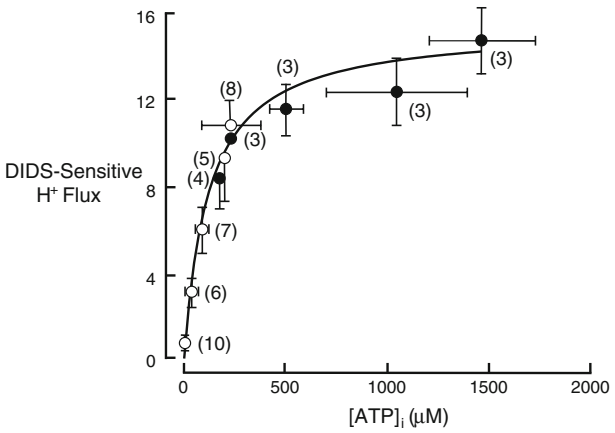

Fig. 2 ATP dependence of Na^+-driven Cl–HCO_3 exchange. Experiments summarized by *open circles* were performed with the same protocol as in Fig. 1, except that the DFs contained no ATP but PEPPA concentrations ranging 0–3 mM. *Closed circles* summarize experiments in which we dialyzed axons with increasing [ATP] in the presence of 3 mM PEPPA. Table 1 summarizes the ATP and PEPPA compositions of the DFs as well as the measured $[ATP]_i$ and J_H values. The curve through the data is the result of a nonlinear least-squares curve fit by the function $V = V_{max} \times S/(S + K_m)$. The best-fit values were 124 ± 19 μM for K_m and 15.6 ± 6.3 pmole cm^{-2} s^{-1} for V_{max}. The number of J_H determinations is given in parentheses, permitting one to correlate the plotted points with the data in Table 1. *Bars*, which represent standard errors, are omitted when the end of the bar would have overlapped with the symbol

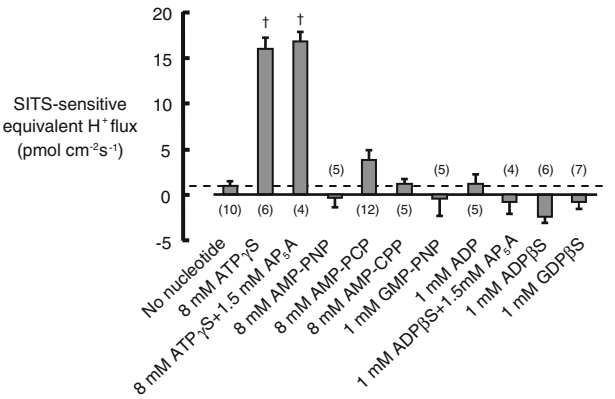

Fig. 3 Effect of nucleotides on Na^+-driven Cl–HCO_3 exchange in the absence of background ATP. Axons were dialyzed as described for Fig. 1, except that the DFs did not contain either ATP or PEPPA. For experiments summarized by the 10 rightmost bars, the DF contained the indicated nucleotide ± AP_5A. Number of experiments is given in parentheses. A one-way ANOVA yielded an overall P of 4 × 10^{-7}. $^{\dagger}P < 0.0001$ by Dunnett's post hoc analysis. Only the data for ATPγS and ATPγS + AP_5A were significantly different from control (i.e., no nucleotide). The mean J_H for AMP-PCP (i.e., 3.8 ± 1.1 pmole cm^{-2} s^{-1}) failed to reach statistical significance ($P = 0.08$)

significantly greater flux, which amounted to 16.0 ± 1.3 pmole cm^{-2} s^{-1}. Because ATPγ may contain some ADP, we also examined the effect of ATPγS in the presence of diadenosine pentaphosphate (AP_5A), a potent

Table 2 HCO_3^--dependent ^{36}Cl efflux from axons dialyzed at pH 6.7[a]

DF	Cl^- efflux (pmol cm^{-2} s^{-1})		
	0 [HCO_3^-]	12 mM [HCO_3^-]	HCO_3^--dependent
0 ATP	8.5 ± 0.7	8.8 ± 0.9	0.3 ± 0.4 (5) NS, paired
4 mM ATP	9.6 ± 0.9	13.2 ± 1.2	3.6 ± 0.4 (7) $P < 0.0001$, paired
8 mM ATPγS	10.7 ± 1.0	15.3 ± 1.3	4.6 ± 0.7 (13) $P < 0.0001$, paired

[a] All data are means ± SEM of unidirectional efflux; number of experiments in parentheses. In each row, the 0- and 12-mM HCO_3^- conditions were compared using a paired *t*-test. The difference in HCO_3^- stimulated ^{36}Cl efflux between 4 mM ATP and 8 mM ATPγS was not statistically significant

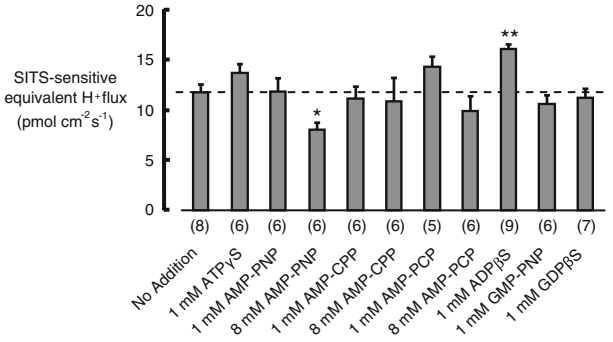

Fig. 4 Effect of nucleotides on Na^+-driven Cl–HCO_3 exchange in the presence of ~230 μM ATP. Axons were dialyzed as described for Fig. 1, except that the DFs contained no ATP but 3 mM PEPPA. Analyses of the extruded axoplasm from each experiment yielded an average of 230 μM [ATP]. For experiments summarized by the 10 rightmost bars, the DF contained the indicated nucleotide. Number of experiments is given in parentheses. A one-way ANOVA yielded an overall *P* of <0.0001. $^*P = 0.045$, $^{**}P = 0.0039$ by Dunnett's post hoc analysis

inhibitor of adenylate kinase (Lienhard and Secemski 1973), which catalyzes the reaction 2 ADP ⇄ ATP + AMP. However, AP_5A did not reduce the ability of ATPγS to support transport. None of the other nucleotide trisphosphate analogues increased J_H significantly above background, as determined by ANOVA. Similarly, none of the nucleotide diphosphates supported Na-driven Cl–HCO_3 exchange.

To address the possibility that the ATPγS effect on acid extrusion was the result of another acid-extrusion process, we measured ^{36}Cl efflux from axons dialyzed at pH 6.7 with solutions that contained either no nucleotides, 4 mM ATP or 8 mM ATPγS. The results (Table 2) show that both the ATP- and ATPγS-treated axons exhibited a higher rate of unidirectional ^{36}Cl efflux when exposed to 12 mM HCO_3^-, whereas in the absence of nucleotide, exposure to 12 mM HCO_3^- had no effect on ^{36}Cl efflux. Previous work has shown that stilbenes block the entire HCO_3^--stimulated ^{36}Cl efflux (Russell and Boron 1976; Boron and Russell 1983).

Effect of Nucleotides on Transport at a Background $[ATP]_i$ of ~230 μM

In a third series of experiments, we asked whether the same nucleotides summarized in Fig. 3 could alter J_H in the presence of an intermediate $[ATP]_i$ that would allow us to detect either a stimulation or an inhibition of transport. In 12 experiments, dialysis with a pH-6.7 fluid containing 3 PEPPA but no added nucleotides produced a J_H of 11.7 ± 0.8 (Fig. 4, leftmost bar and sixth data row in Table 1). The measured $[ATP]_i$ in this group of axons was 231 μM (Table 1)—about twice the apparent K_m. We added nucleotides to this DF at either 1 or 8 mM. Dialysis with 8 mM—but not with 1 mM—AMP-PNP modestly reduced J_H to 8.0 ± 0.6 pmol cm^{-2} s^{-1}. On the other hand, 1 mM ADPβS modestly increased J_H to 16.0 ± 0.5 pmol cm^{-2} s^{-1}.

Discussion

ATP Dependence of Na^+-Driven Cl–HCO_3 Exchange

One of the first-described characteristics of the Na-driven/Cl–HCO_3 exchanger was its ATP dependence in the squid giant axon. Here, we have determined that the apparent K_m for ATP is ~124 μM, more than an order of magnitude lower than the axon's physiological $[ATP]_i$ of ~4 mM (Brinley and Mullins, 1967). Of course, we obtained this K_m value under a very specific set of conditions, and it might very well depend on such parameters as pH and ion gradients. Nevertheless, 124 μM is within the range of values for other ATP-dependent processes in the squid axon and elsewhere. For example, in the squid axon, the apparent K_m is 86 μM for the Na/K/Cl cotransporter (Altamirano et al. 1988), 250 μM for the Na–Ca exchanger (Di Polo 1977) and 200 μM for the Na–K pump (Beauge and Di Polo 1981).

Comparison of Equivalent H^+ Flux vs. ^{36}Cl Efflux

A Na-dependent Cl–HCO_3 exchanger would have a stoichiometry of two H^+ equivalents extruded for each Cl^- extruded. Given HCO_3^--dependent ^{36}Cl efflux of ~4.6 ± 0.7 pmole cm^{-2} s^{-1} in the presence of 8 mM ATPγS (Table 2), we might have expected an equivalent H^+ flux of ~9.2 pmole cm^{-2} s^{-1} if $[Cl^-]_i$ were only 150 mM (as in the ^{36}Cl experiments), but ~11.8 pmol cm^{-2} s^{-1}

when we recall that $[Cl^-]_i$ was in fact 400 mM in the pH_i experiments. In fact, for the data in Fig. 2, in which ATP supported transport, the V_{max} was an equivalent H^+ flux of 15.6 ± 6.3 pmole cm^{-2} s^{-1}. In Fig. 3, ATPγS supported 16.0 ± 1.3 pmole cm^{-2} s^{-1}. The agreement between the predicted and observed values is not unreasonable for two reasons. First, we obtained the ^{36}Cl data during continuous dialysis but were forced to halt dialysis for the pH_i experiments (Fig. 1). Second, the computed equivalent H^+ flux is proportional to the computed buffering power. In fact, if cytosolic components—which have a relatively low natural buffering power (Boron and De Weer 1976b)—diluted the DF, the true closed-system buffering power would have been somewhat less than the computed buffering power of the DF, leading to an overestimate of H^+ flux. Note, however, that any error in buffering power (i.e., scaling of the computed equivalent H^+ flux) would not affect the computed K_m for ATP.

Potential Role of ATP

An earlier study with ATPγS (Boron et al. 1988) demonstrated that the squid axon's Na^+-driven Cl–HCO_3 exchanger does not use ATP as fuel. One potential mechanism by which low $[ATP]_i$ could inhibit Na^+-driven Cl–HCO_3 exchange would be if, by catalyzing the reaction 2 ADP → ATP + AMP, adenylate kinase would release AMP that would activate AMP kinase, which in turn would block various energy-depleting processes (for review, see Young et al. 2005)—presumably including the Na^+-driven Cl–HCO_3 exchanger. However, it is not clear how ATPγS could relieve this inhibition except by inhibiting either of the two aforementioned kinases.

One goal of the present study was to rule out one of the remaining hypotheses, namely, that ATP (or ATPγS) promotes transport by either (1) binding to an ATP-binding site or (2) phosphorylating the transporter (or an essential activator). If ATP (or ATPγS) worked via an ATP-binding site, then it would be reasonable to expect that AMP-PNP or AMP-PCP should also bind to the activating site and support transport. Indeed, others have reported that AMP-PNP binds to the cystic fibrosis transmembrane conductance regulator (CFTR) (Hwang et al. 1994; Gunderson and Kopito 1994) and that AMP-PCP inhibits a Cl^- channel in zymogen granules (Thevenod et al. 1994). However, we found that neither of these two nonhydrolyzable ATP analogues could support transport, making the binding hypothesis unlikely. Moreover, the cloned squid Na^+-driven Cl–HCO_3 exchanger sqNDCBE (Virkki et al. 2003) does not have a consensus nucleotide-binding site.

Regarding the phosphorylation hypothesis, it is well established that ATPγS leads to phosphatase-resistant protein phosphorylation (Cassel and Glaser 1982). Other investigators, in studies on membrane proteins, have exploited the stable phosphorylation produced by ATPγS (Wu et al. 2001). Moreover, sqNDCBE (Virkki et al. 2003), on either its cytoplasmic N or C terminus, has multiple protein kinase A and protein kinase C consensus phosphorylation sites, though we do not know whether the phosphorylation state of any of these affects transporter function. We suggest that the most likely hypothesis is that ATPγS similarly leads to the stable phosphorylation of either the Na^+-driven Cl–HCO_3 exchanger protein or an essential activator.

Two intriguing observations were that, in the presence of a background $[ATP]_i$ of ~230 μM, 8 mM AMP-PNP caused a significant decrease in J_H, whereas 1 mM ADPβS caused a significant increase (Fig. 4). In principle, AMP-PNP could have inhibited transport by competing with ATP for binding to a hypothetical ATP-binding site. However, because AMP-PNP failed to support transport in the nominal absence of ATP (Fig. 3), we think it is more likely that AMP-PNP inhibited a kinase. In principle, ADPβS could have stimulated transport by binding to a hypothetical ATP-binding site. However, because ADPβS (like AMP-PNP) failed to support transport in the nominal absence of ATP (Fig. 3), we think it is more likely that ADPβS somehow promoted phosphorylation. For example, the axon could have converted ADPβS via adenylate kinase to ATPβS. The γ phosphate of ATPβS (compared to that of ATPγS) is structurally more similar to the γ phosphate of ATP and, thus, might have a higher affinity for the kinase.

Acknowledgments This work was supported by National Institutes of Health grants NS18400 and NS11946. We thank Mr. Mike Hernandez for assistance in performing the ATP assays and Mr. Duncan Wong for technical assistance.

References

Altamirano AA, Breitwieser GE, Russell JM (1988) Vanadate and fluoride effects on Na^+-K^+-Cl^- cotransport in squid giant axon. Am J Physiol 254:C582–C586

Altamirano AA, Breitwieser GE, Russell JM (1995) Effects of okadaic acid and intracellular Cl^- on Na^+-K^+-Cl^- cotransport. Am J Physiol 269:C878–C883

Beauge L, Di Polo R (1981) The effects of ATP on the interactions between monovalent cations and the sodium pump in dialysed squid axons. J Physiol 314:457–480

Boron WF (1985) Intracellular-pH-regulating mechanism of the squid axon: relation between the external Na^+ and HCO_3^- dependences. J Gen Physiol 85:325–345

Boron WF (1989) Cellular buffering and intracellular pH. In: The regulation of acid-base balance. Raven Press, New York, pp 33–56

Boron WF, De Weer P (1976a) Active proton transport stimulated by CO_2/HCO_3^- blocked by cyanide. Nature 259:240–241

Boron WF, De Weer P (1976b) Intracellular pH transients in squid giant axons caused by CO_2, NH_3 and metabolic inhibitors. J Gen Physiol 67:91–112

Boron WF, Hogan E, Russell JM (1988) pH-sensitive activation of the intracellular-pH regulation system in squid axons by ATP-g-S. Nature 332:262–265

Boron WF, Knakal RC (1985) Intracellular-pH regulation by the squid axon: competition of DNDS, a reversible stilbene derivative, with external Na^+ and HCO_3^-. Biophys J 47:490a

Boron WF, Knakal RC (1989) Intracellular pH-regulating mechanism of the squid axon: interaction between DNDS and extracellular Na^+ and HCO_3^-. J Gen Physiol 93:123–150

Boron WF, Russell JM (1983) Stoichiometry and ion dependencies of the intracellular-pH-regulating mechanism in squid giant axons. J Gen Physiol 81:373–399

Brinley FJ Jr, Mullins LJ (1967) Sodium extrusion by internally dialyzed squid axons. J Gen Physiol 50:2303–2331

Cassel D, Glaser L (1982) Resistance to phosphatase of thiophosphorylated epidermal growth factor receptor in A431 membranes. Proc Natl Acad Sci USA 79:2231–2235

Di Polo R (1977) Characterization of the ATP-dependent calcium efflux in dialyzed squid giant axons. J Gen Physiol 69:795–813

Gunderson KL, Kopito RR (1994) Effects of pyrophosphate and nucleotide analogs suggest a role for ATP hydrolysis in cystic fibrosis transmembrane regulator channel gating. J Biol Chem 269:19349–19353

Hinke JAM (1967) Cation-selective microelectrodes for intracellular use. In: Glass electrodes for hydrogen and other cations. Principle and Practice. Dekker, New York, pp 464–477

Hwang TC, Nagel G, Nairn AC, Gadsby DC (1994) Regulation of the gating of cystic fibrosis transmembrane conductance regulator Cl channels by phosphorylation and ATP hydrolysis. Proc Natl Acad Sci USA 91:4698–4702

Lienhard GE, Secemski II (1973) P1,P5-di(adenosine-5′)pentaphosphate, a potent multisubstrate inhibitor of adenylate kinase. J Biol Chem 248:1121–1123

Roos A, Boron WF (1981) Intracellular pH. Physiol Rev 61:296–434

Russell JM, Boron WF (1976) Role of chloride transport in regulation of intracellular pH. Nature 264:73–74

Thevenod F, Anderie I, Schulz I (1994) Monoclonal antibodies against MDR1 P-glycoprotein inhibit chloride conductance and label a 65-kDa protein in pancreatic zymogen granule membranes. J Biol Chem 269:24410–24417

Thomas RC (1976) Ionic mechanism of the H^+ pump in a snail neurone. Nature 262:54–55

Thomas RC (1977) The role of bicarbonate, chloride and sodium ions in the regulation of intracellular pH in snail neurones. J Physiol 273:317–338

Virkki LV, Choi I, Davis BA, Boron WF (2003) Cloning of a Na^+-driven Cl/HCO_3 exchanger from squid giant fiber lobe. Am J Physiol 285:C771–C780

Wu JV, Joo NS, Krouse ME, Wine JJ (2001) Cystic fibrosis transmembrane conductance regulator gating requires cytosolic electrolytes. J Biol Chem 276:6473–6478

Young LH, Li J, Baron SJ, Russell RR (2005) AMP-activated protein kinase: a key stress signaling pathway in the heart. Trends Cardiovasc Med 15:110–118